Unusual effects in the propagation of ultrasonic shear waves in crystals exhibiting internal strains

1993 J. Phys.: Condens. Matter 5 4391

(http://iopscience.iop.org/0953-8984/5/26/011)

J. Phys.: Condens. Matter 5 (1993) 4391–4400. Printed in the UK

Unusual effects in the propagation of ultrasonic shear waves in crystals exhibiting internal strains

F Michard

Laboratoire de Recherches Physiques (associé au CNRS), Tour 22, Université Pierre et Marie Curie, 4 place Jussieu, 75252 Paris Cedex 05, France

Received 22 February 1993

Abstract. Unusual effects are observed when ultrasonic shear waves are propagated in some specific directions of $Pb(NO_3)_2$ and CaF_2 single crystals. $Pb(NO_3)_2$ and CaF_2 are centrosymmetric crystals in which not all the ions are at the centre of inversion of the lattices. Consequently, internal strains exist which can be coupled with external deformation modes. In this paper the unusual behaviour of ultrasonic propagation is described and tentatively interpreted in terms of a coupling between macroscopic modes assisted by internal strains.

1. Introduction

When a crystal is elastically deformed, an internal strain can be induced. This strain is due to relative shifts between the different Bravais sublattices. Such shifts, as pointed out by Born and Huang [1], are microscopic in magnitude and do not affect the macroscopic dimensions of a specimen.

It is fairly evident that internal strains do not exist when all the particles of the crystal are located at the centre of inversion of the lattice. On the contrary, internal and external deformations exist and can be coupled in crystals in which not all the ions are at the centre of inversion of the lattice.

One of the simplest crystalline lattices in which such internal strains may be induced is the fluorite lattice (CaF_2). This crystalline network consists of three interpenetrating Bravais lattices of identical face-centred cubic structure. Although the point symmetry group $m3m$ possesses a centre of inversion, only the calcium ions are located at lattice points which are a centre of inversion of the lattice. When the crystal is submitted to some macroscopic shear strains, both sublattices consisting of non-homologous fluorine ions experience a relative shift. This internal strain exhibits the same symmetry as the optical phonon which accounts for the Raman scattering [2].

Let us look, for instance, at the effect on the fluorine ions of a macroscopic shear strain lying in the Ox_1x_2 plane as induced by an ultrasonic wave propagating along [010] (Ox_2) and vibrating along [100] (Ox_1). Figure 1(a) shows one eighth of the fluorite cubic cell. The shear strain is equivalent to a compression and an expansion along the bisectrixes of Ox_1, Ox_2. Submitted to this strain the fluorine ion shifts along [001] (Ox_3), thereby keeping equal the distances between its new location and the neighbouring calcium ions. Looking at the adjacent cell (figure 1(b)) the centre of which is occupied by a fluorine ion belonging to the other Bravais lattice, it shifts along Ox_3 in the opposite sense when it experiences the same macroscopic strain.

0953-8984/93/264391+10$07.50

Until now, to our knowledge, little attention has been paid to specific aspects of ultrasonic propagation in crystals exhibiting internal strains. In this paper, experimental results concerning the measurement of ultrasonic attenuation in such crystals are reported.

In section 2 the experimental technique and the description of the investigated crystal are presented. In section 3, experimental results are reported. Finally the anomalous ultrasonic attenuation found in $Pb(NO_3)_2$ is discussed and tentatively interpreted in terms of a transfer of energy from mode to mode assisted by internal strains.

2. Experimental details

The experimental technique that we have used to measure the ultrasonic attenuation is an acousto-optic technique [3]. The acousto-optic interaction occurs between a laser beam and the ultrasonic wave generated in the crystal. In the ultrasonic frequency range considered, the light is scattered at the Bragg angle. This technique allows us to obtain local knowledge of the macroscopic elastic response. In this way, it appears to be a suitable technique for studying the internal strains induced by the ultrasonic waves.

A schematic arrangement for studying acousto-optic interaction is shown in figure 2. Shear ultrasonic pulses are generated in the frequency range 100 MHz–1 GHz by a lithium niobate transducer which is driven by a RF pulse generator. Rotating the transducer allows us to change the ultrasonic wave polarization. The light source is a He–Ne laser with a power output of 7 mW. The light scattered at the Bragg angle by the ultrasonic wave is detected by a photodiode and displayed on an oscilloscope.

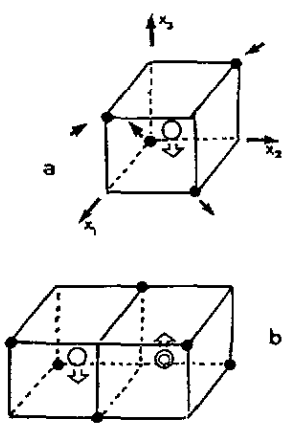

Figure 1. Internal strain in a fluorite cell under stress in the (x_1, x_2) plane, sharing (a) one eighth of the cubic cell and (b) two adjacent cells: ○ ◎ fluorine; ●, calcium.

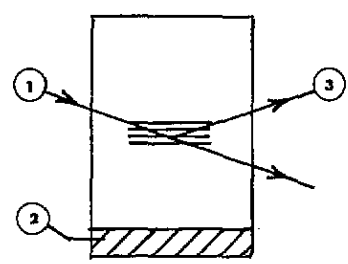

Figure 2. Acousto-optic interaction: the incident laser beam 1 is diffracted by the ultrasonic waves generated by a lithium niobate transducer 2; then the diffracted light beam is detected by a photodiode 3.

Over the frequency range explored, the Bragg angle is very small (1–2°) so that the incident and diffracted light beams are nearly perpendicular to the acoustic wavevector. The intensity of the diffracted beam is given by $I = I_0 \sin^2(AP^{1/2})$, where I_0 is the intensity of the incident beam, A is a constant whose value depends on the crystal studied and P is

the acoustic power. For low acoustic powers (say $I/I_0 < 3 \times 10^{-2}$), the intensity of the diffracted beam is proportional to the acoustic power to within an error of 1%.

The measurement of the diffracted light intensity I as a function of the distance d from the transducer allows one to obtain the ultrasonic attenuation with an accuracy of the order of 1% [4]. For instance, a plot of $\log I$ versus d is shown in figure 3 in the case of a longitudinal ultrasonic wave propagating along [100] in a lead nitrate crystal. On account of the ultrasonic attenuation, the diffracted light intensity—which is proportional to the acoustic intensity—exponentially decreases, moving off from the transducer and, consequently, $\log I$ decreases linearly.

3. Results

The crystal that we have selected to study is lead nitrate ($Pb(NO_3)_2$). In this crystal, the anions do not occupy centres of inversion in the crystalline lattice. Submitted to some shear strains, both lattices consisting of non-homologous NO_3^- ions experience a relative shift. On account of the large polarizability of the ions of the crystalline lattice, the part played by the internal deformation in the macroscopic elastic response is easier to demonstrate in this crystal.

The lead nitrate structure is very similar to the fluorite structure. This crystal belongs to the cubic system and exhibits $m3$ symmetry. One eighth of the cubic cell is shown in figure 4. The Pb^{2+} ions are located in the same position as the Ca^{2+} ions in the fluorite lattice (figure 5). The complex ion NO_3^-, which is large, is shifted with respect to the central position occupied by the F^- ion, along one of the [111] directions towards the vacuum vertex.

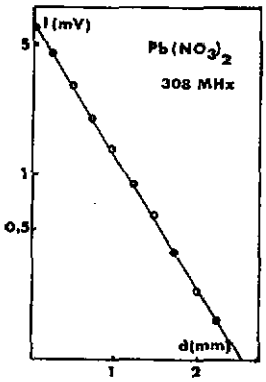

Figure 3. Ultrasonic wave damping in the case of a longitudinal wave propagating along [100] in a lead nitrate crystal.

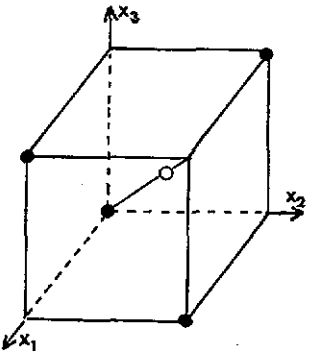

Figure 4. Lead nitrate structure sharing one eighth of the cubic cell: ●, Pb^{2+}; ○, NO_3^-.

We have studied the behaviour of the diffracted light intensity along the ultrasonic path in a lead nitrate crystal for several ultrasonic frequencies. The sample is a parallelepiped, oriented along [010] (Ox_2) and the bisectrixes of Ox_1 and Ox_3: [101] (Ox_1') and [$\bar{1}$01] (Ox_3').

The arrangements selected for the acousto-optic interaction are the following: the acoustic wavevector is parallel to Ox_2 and the incident light beam parallel to Ox_1'; the

ultrasonic wave polarization is parallel to Ox_3' (case (*a*)) or parallel to Ox_1' (case (*b*)). The behaviour of the diffracted light intensity I, as a function of the ultrasonic path d, is shown in figure 6 in case (*a*) (polarization of the transducer perpendicular to the laser beam). The value of the ultrasonic frequency is 534 MHz. Firstly, we may observe that the diffracted light intensity is very large, of the same order as in the case of acousto-optic diffraction by ultrasonic longitudinal waves, for the same level of the acoustic power. More surprising is the occurrence of regular oscillations of the diffracted light intensity superposed on a term which depends linearly on d and corresponds to the ultrasonic attenuation as reported in figure 3. This curve is compared in figure 7 with the curve that we obtained in case (*b*): ultrasonic polarization parallel to Ox_1' (parallel to the laser beam), the value of the ultrasonic frequency being 518 MHz. This frequency is slightly different from 534 MHz because of the easiest electrical matching conditions. This arrangement for the acousto-optic interaction is in fact not allowed by the selection rules in the case of a crystal belonging to cubic symmetry. Furthermore, the diffracted light intensity exhibits oscillations such that this curve is *complementary* to the curve that we obtained in case (*a*), the maximum of one corresponding to the minimum of the other. In the two cases, we have subtracted from the experimental results the contribution occurring from the *classical* ultrasonic wave damping.

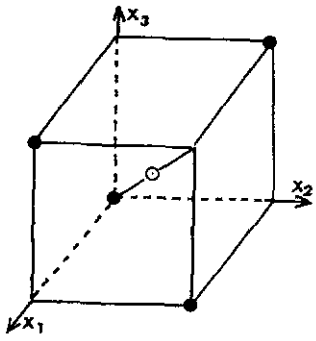

Figure 5. Fluorine structure sharing one eighth of the cubic cell: ●, Ca^{2+}; ○, F^-.

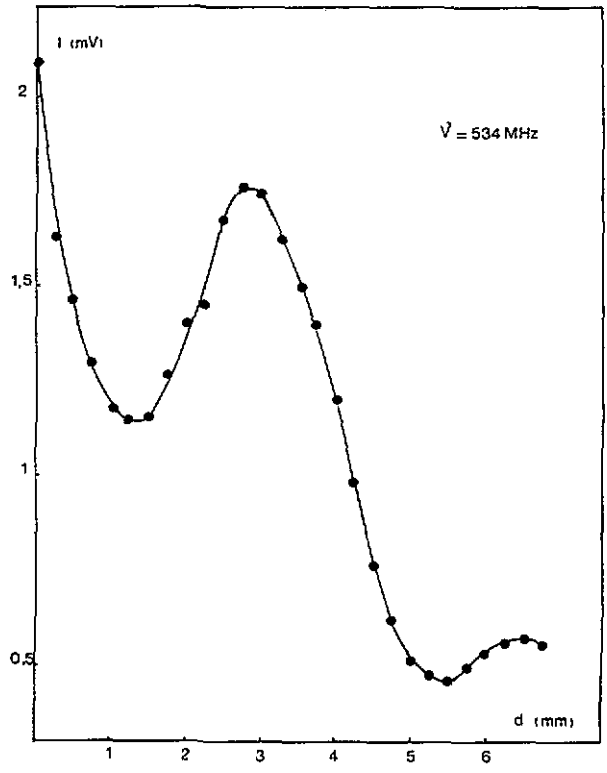

Figure 6. Behaviour of the diffracted light intensity I as a function of the distance d from the transducer for the following acousto-optic arrangement: wavevector parallel to [010] (Ox_2); incident laser beam parallel to [101] (Ox_1'); polarization of the transducer parallel to $[\bar{1}01]$ (Ox_3'); case (*a*); $\nu = 534$ MHz.

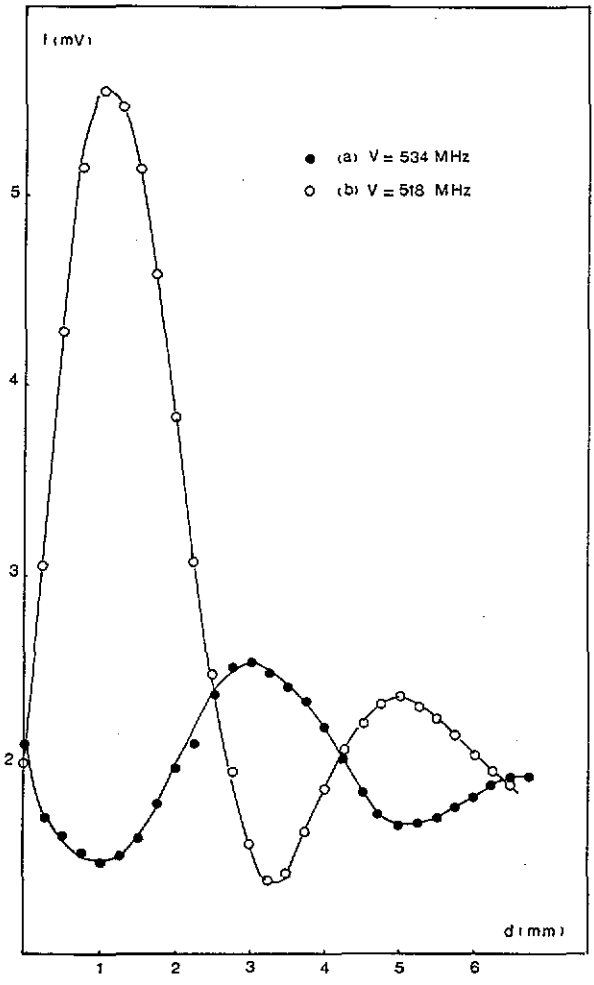

Figure 7. Comparison between the curves $I = f(d)$ in the case of the following acousto-optic arrangements: ●, case (a), polarization of the transducer perpendicular to the laser beam, $\nu = 534$ MHz; ○, case (b), polarization of the transducer parallel to the laser beam, $\nu = 518$ MHz.

For ultrasonic frequencies smaller than about 650 MHz, the diffracted light intensity oscillations are displayed over the whole sample length.

Comparing the previous curves (figure 7) with those that we obtained in the case of two other ultrasonic frequencies ν (628 and 636 MHz in figure 8 and 346 and 343 MHz in figure 9) and for the same experimental conditions (transducer polarization perpendicular, i.e. case (a), and parallel, i.e. case (b), to the laser beam), we observed that increasing the ultrasonic frequency involves a simultaneous decrease in the spectral period of the oscillations. The spatial period depends linearly on the inverse of the ultrasonic frequency ν. These experimental results demonstrate that a *balancing* of the acoustical energy between the two shear modes exists, the polarization of which is in one case parallel to Ox_3' (case (a)) and in the other case parallel to Ox_1' (case (b)). In figure 10 is displayed the behaviour of Δ_1, the first interval observed moving off from the transducer, between a maximum and a minimum of the diffracted light intensity over the frequency range 340–980 MHz. Increasing the ultrasonic frequency ν by a 100 MHz step, we observe a simultaneous decrease in Δ_1 of the order of 0.5 mm.

These experimental results show a linear coupling between the two macroscopic shear modes, the corresponding displacements involved being along the bisectrixes of [100] and

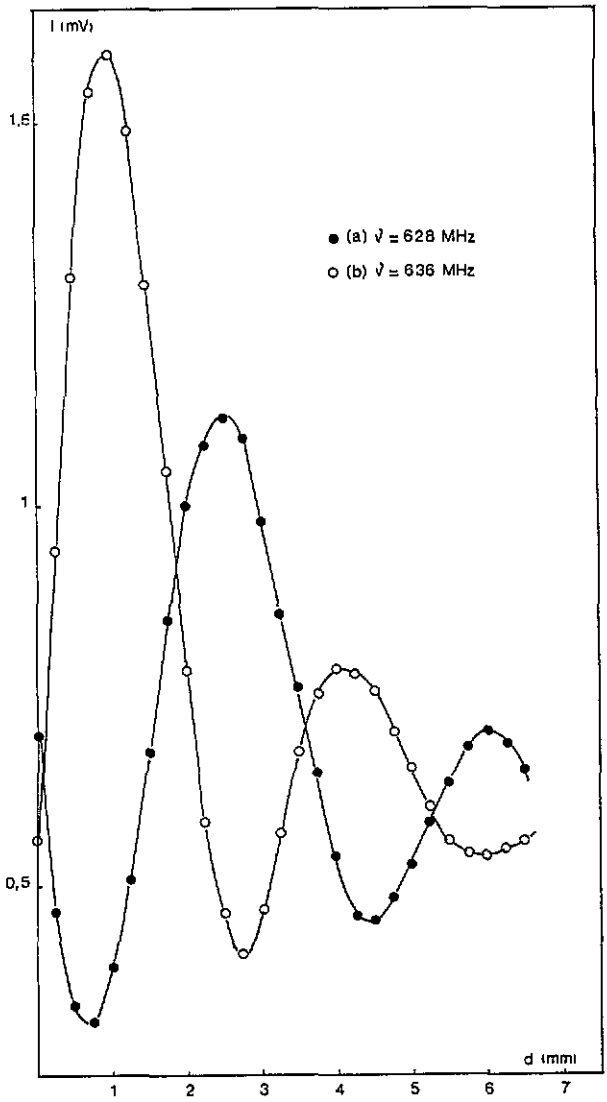

Figure 8. Comparison between the curves $I = f(d)$ in case (a) ($\nu = 628$ MHz) (●) and case (b) ($\nu = 636$ MHz) (○).

[001] (wavevector parallel to [010]). Such a coupling, which does not occur in crystals if the lattice structure is such that every ion occupies a centre of inversion, probably involves the internal strain mode induced by the macroscopic shear modes (external modes) in the case of the $Pb(NO_3)_2$ crystals.

Similar effects can be observed when elastic shear waves are propagated in CaF_2 single crystals. However, the polarizabilities of Ca and F ions are small and the anomalous effects which are shown in figure 11 are not so large as in $Pb(NO_3)_2$. So we shall limit the discussion to this latter case.

4. Discussion

We would like to make the following comment: in the case of an ultrasonic shear wave propagating along [010] (Ox_2), the polarization of which is parallel to $[\bar{1}01]$ (Ox_3') or

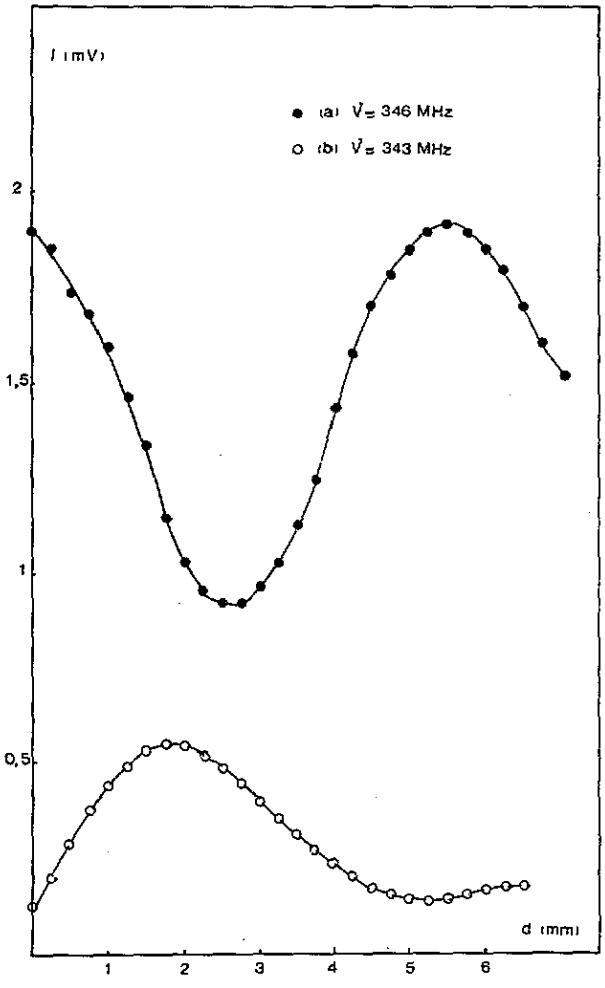

Figure 9. Comparison between the curves $I = f(d)$ in case (a) ($\nu = 346$ MHz) (●) and case (b) ($\nu = 343$ MHz) (○). In case (b), the acousto-optic power is 1.6 times lower than in case (a).

to [101] (Ox_1') (case (a) or (b), respectively), the NO_3^- displacement associated with the internal mode is parallel to the shear macroscopic vibration (if the lattice structure model is the fluorite type). The internal strain in this case is different from that described in figure 1 but can be easily inferred from this last example.

From the viewpoint of a microscopic approach it may be interesting to express the coupling intensity between the displacements of the NO_3^- ions belonging to the adjacent elementary cells (figure 12) in terms of the interatomic force constants, k describing the Pb^{2+}–NO_3^- interactions and k' the NO_3^-–NO_3^- interactions. The very elementary model that we describe now allows us to connect the coupling intensity to the spatial period of the energy exchange observed in the experiments previously reported. The NO_3^- displacements X_1 and X_2 result in this scheme from the superposition of two normal modes:

(1) simultaneous translation impressed by the macroscopic shear external mode with the frequency $\Omega_1 = \sqrt{k/m}$;

(2) opposite motion to one another of the two NO_3^- ions, as happens in the case of an internal mode as a consequence of the macroscopic shear mode, with the frequency $\Omega_2 = \sqrt{(k + 2k')/m}$.

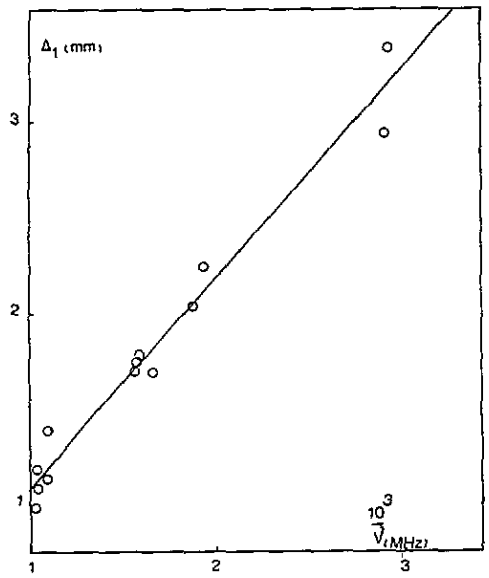

Figure 10. Behaviour of Δ_1, the first interval measured moving off from the transducer between a maximum and a minimum of the diffracted light intensity, as a function of $1/\nu$ (ν is the ultrasonic frequency).

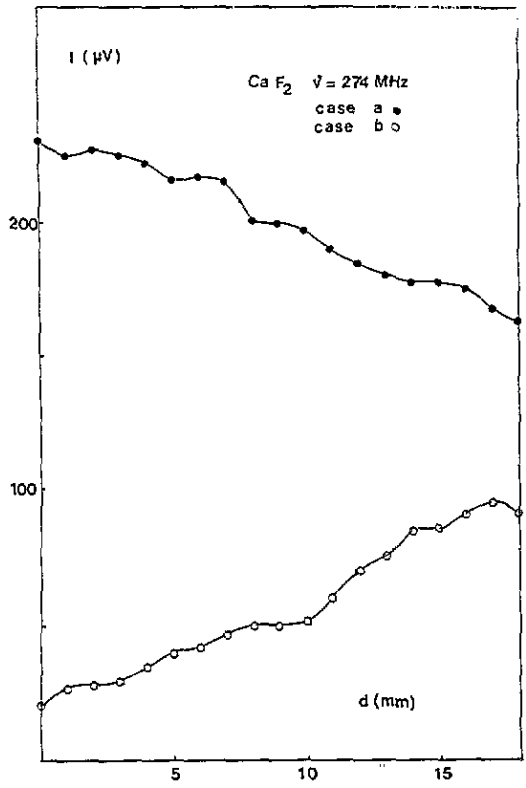

Figure 11. Acousto-optic interaction in a fluorite crystal CaF_2. Comparison between the curves $I = f(d)$ in the case of the following acousto-optic arrangement: wavevector parallel to [010] (Ox_2); laser beam parallel to [100] (Ox_1); ●, case (*a*), polarization of the transducer parallel to [001] (Ox_3) (perpendicular to the laser beam) $\nu = 274$ MHz; ○, case (*b*), polarization of the transducer parallel to [100] (Ox_1) (parallel to the laser beam), $\nu = 274$ MHz.

The NO_3^- displacements X_1 and X_2 exhibit a beating behaviour:

$$X_1 \propto \cos(\tfrac{1}{2}K\omega t)\cos(\omega t)$$

$$X_2 \propto \sin(\tfrac{1}{2}K\omega t)\sin(\omega t)$$

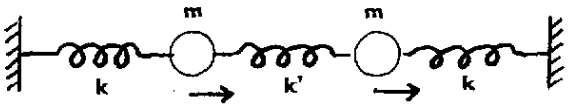

Figure 12. Two identical masses m and springs (spring constant k) making up two identical oscillators connected by a spring (spring constant k'). X_1 and X_2 correspond to the displacements of the two masses.

where K is the coupling coefficient given by $K = k'/(k + k')$, and $\omega^2 = (k + k')/m$ and where we suppose that $k' \ll k$.

In the case of the acousto-optic experiments, the diffracted light intensity is proportional to the acoustic power and the distance between a maximum and a minimum of the intensity is $\frac{1}{4}\Lambda = \Delta$, where Λ is the spatial period of the oscillating signal. If V is the phase velocity of the travelling displacements, the beating frequency f is such that $f = V/\Lambda = \frac{1}{2}Kv$ (v is the ultrasonic frequency).

The experimental knowledge of f allows us to estimate the coupling coefficient K. If the internal strains mainly depend on the short-range interactions between the ions, it is possible to evaluate $K \simeq k'/k$ by means of a very simple model [5, 6]. In this model we suppose that the crystalline lattice is the same as the fluorite lattice. The force constant k results from interactions between the cation and the anion located at the distance $r_{+-} = a\sqrt{3}/4$ (a is the lattice parameter); the force constant k' results in the case of nitrate crystals from interactions between NO_3^- ions located along the [111] axis; the distance between neighbours is $r_{--} = a\sqrt{3}/2$ (to preserve the analogy exhibited by the internal strain mode and the optical lattice mode). The results that we obtained are given in table 1 for lead nitrate and for some other isomorphous crystals.

Table 1. Results obtained for lead nitrate and isomorphous crystals. For Λ_{th} and Λ_{exp}, $\nu = 500$ MHz.

	r_{+-} (Å)	r_{--} (Å)	$K_{th} \simeq k'/k$	Λ_{th} (mm)	Λ_{exp} (mm)	K_{exp}
$Pb(NO_3)_2$	3.40	6.80	7.7×10^{-4}	9.0	8.2	8.4×10^{-4}
$Sr(NO_3)_2$	3.37	6.74	1.1×10^{-3}	8.1		
$Ba(NO_3)_2$	3.51	7.02	3.9×10^{-5}	203		

The theoretical values of Λ, the beating spatial period, obtained in the case of lead nitrate is compared with the period of the modulation of the diffracted light intensity observed in the experiments previously described. Both results are sufficiently in agreement to strengthen the opinion that the internal strain mode is involved in the coupling mechanism which occurs between the macroscopic strain modes, if the lattice structure is such that every ion does not occupy a centre of inversion.

Acknowledgments

The author is indebted to Professor A Zarembowitch and to Professor A Maradudin for their interest in this work and fruitful discussions.

References

[1] Born M and Huang K 1954 *Dynamical Theory of Crystal Lattices* (Oxford: Oxford University Press)

[2] Cribier D 1959 *Ann. Phys., Paris* 4 333
[3] Korpel A 1972 *Applied Solid State Science* vol 3 (New York: Academic) pp 72–175
[4] Michard F 1981 *Phys. Rev.* B **24** 4253
[5] Reitz J R, Seitz R N and Genberg R W 1961 *J. Phys. Chem. Solids* **19** 73
[6] Michard F 1973 *Thèse d'Etat* Université de Paris